DOI 10.1007/s10812-017-0423-5
Journal of Applied Spectroscopy, Vol. 84, No.1, March, 2017 (Russian Original Vol. 84, No. 1, January–February, 2017)

LASER-INDUCED BREAKDOWN SPECTROSCOPY AND PLASMA CHARACTERIZATION GENERATED BY LONG-PULSE LASER ON SOIL SAMPLES

S. Xu,* W. Duan, R. Ning, Q. Li, and R. Jiang

UDC 621.373.8;533.9

The plasma is generated by focusing a long-pulse (80 μs) Nd:YAG laser on chromium-doped soil samples. The calibration curves are drawn using the intensity ratio of the chromium spectral line at 425.435 nm with the iron spectral line (425.079 nm) as reference. The regression coefficient of the calibration curve is 0.993, and the limit of detection is 16 mg/kg, which is 19% less than that for the case of a Q-switched laser In the method of long-pulse laser-induced breakdown spectroscopy, the laser-induced plasma had a temperature of 15795.907 K and an electron density of 2.988×10^{17} *cm*$^{-3}$*, which exceeded the corresponding plasma parameters of the Q-switched laser-induced breakdown spectroscopy by 75% and 24% respectively.*

Keywords: *laser-induced breakdown spectroscopy, plasma temperature, electron density, limit of detection.*

Introduction. Laser induced breakdown spectroscopy (LIBS) has advantages such as no requirement for sample preparation, rapid analysis, and on-line analysis in hostile environments, showing extensive potential applications in the field of environmental monitoring [1], geological analysis [2], biomedicine [3], etc. However, the LIBS technique still has vulnerabilities such as strong background intensity and low signal-to-noise ratio compared to conventional approaches (ICP–AES, AAS, etc.) [4, 5]. In recent years, a lot of work has been done to enhance the sensitivity of LIBS [6, 7]. Guo et al. [8] confined plasmas of pure metal and alloyed samples by using a pair of permanent magnets and an aluminum hemispherical cavity. Enhancement factors of only about 11 and 12 in the emission intensity of Co and Cr lines were obtained just with the cavity, while high enhancement factors of about 22 and 24 were acquired with both confinements. Babar Rashid et al. [9] investigated the effect of a double-pulsed configuration on the signal intensity enhancement, and nearly two times signal enhancement was obtained in the collinear double-pulsed configuration and nearly 12 times in the orthogonal configuration as compared to the single-pulse LIBS. However, all these procedures to enhance the effect of LIBS were based on complicated experimental configurations that reduced the advantages of LIBS.

In the present study, both long-pulse and Q-switched laser were employed to induce plasmas of chromium-doped reference soil samples. Ratio calibration curves and limit of detection of chromium (Cr) were obtained. Excitation temperature and electron density of plasma were measured. Data on the signal enhancement and the effect of long-pulse LIBS on plasma characteristics are presented.

Experimental. The schematic diagram of the experimental setup applied for the comparison of long-pulse laser and Q-switched laser configurations is described elsewhere [10]. A long-pulse (pulse energy 325 mJ, pulse width 80 μs) and a Q-switched (pulse energy 67.6 mJ, pulse width 18 ns) Nd:YAG lasers (λ = 1064 nm) were respectively focused by a quartz lens (f = 100 mm) on the surface of Cr-doped reference soil samples. The light emitted from the plasma was collected with an optical fiber and imaged into a grating spectrometer (Andor SR-750-A-R spectrometer) with a charge coupled device (ICCD, Andor, iStar DH3). The spectrometer has a grating of 1200 lines/mm with a slit width of 0.06 mm. The spectrometer and laser were controlled with the help of computer software (Andor solis). The gate delays of the spectrometer are 120 and 175 μs for the long-pulse laser and the Q-switched laser respectively, which was set based on the highest signal-to-background value in both configurations. The gate width is 2 μs and the repetition rate of laser is 1 Hz. According to the quality criteria of the soil environment allowed (GB15618-2008) [11], the limit of Cr is 90, 350, and 400 mg/kg in natural, second type, and

*To whom correspondence should be addressed.

College of Science, Shenyang Ligong University, Liaoning 110159, China; e-mail: dwz_ruoyi@sina.com. Published in Zhurnal Prikladnoi Spektroskopii, Vol. 84, No. 1, pp. 44–48, January–February, 2017. Original article submitted October 19, 2015.

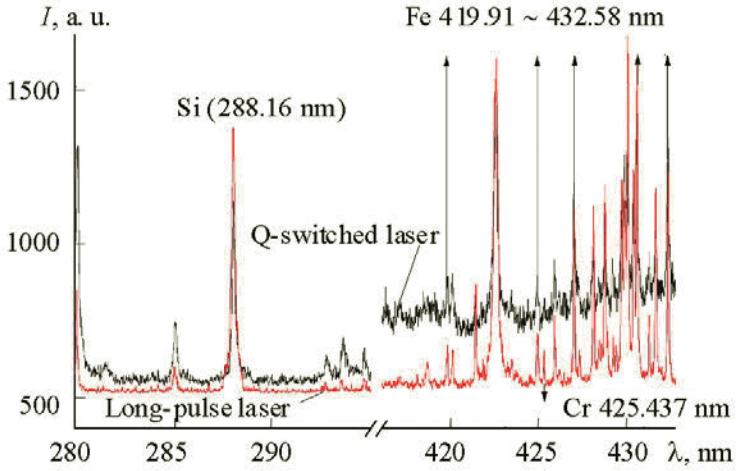

Fig. 1. Comparison of the spectral signal intensities from No. 1 sample induced by long-pulse and Q-switched lasers.

third type of soils, respectively. The fresh soil in the present study was collected from Hunnan District, Shenyang, Liaoning Province, and dried and sieved to a mesh size of 100. The soil was treated with a solution of $Cr(NO_3)_2$ and dried, then doped with a saturated sugar solution and dried at 333.15 K in a drying oven. The prepared soil, containing a specific impurity with a concentration of 50–800 mg/kg, was formed into pellets (diameter 10 mm, thickness 4 mm) under a pressure of 13 MPa. The contents of doped Cr are 50, 100, 200, 400, and 800 mg/kg in soil samples No. 1–5, respectively.

Results and Discussion. Plasmas of soil samples were generated by a long-pulse laser and a Q-switched laser. Emission spectra lines of Si I 288.158 nm, Fe I 419.910 nm, 425.079, 427.176, 430.790, and 432.576 nm, and Cr I 425.435 nm were observed. The spectral intensity of No. 1 sample induced by the long-pulse and Q-switched lasers is shown in Fig. 1. The signal intensity of background generated by the long-pulse laser is more smooth and stable compared to that produced by the Q-switched laser. The signal-to-background ratio and line sharpness of the spectra are enhanced in long-pulse laser configuration. These results indicate that a clear enhancement of signal-to-background ratio occurred with the long-pulse laser configuration of sample No. 1 with 0.005% (50 mg/kg) Cr-doped.

Calibration curves. The ratio calibration curve has been used in quantitative analysis of LIBS to improve the accuracy and decrease the matrix effect on the result of analysis [12]. In the present study, Fe I 425.079 nm is employed as reference line. It does not interfere with the analysis line, and the content of Fe in the sample is stable. The intensity ratios of the spectral line of Cr I at 425.435 nm with the reference line in long-pulse and Q-switched configurations are used in the calibration curves, which are exhibited in Fig. 2. Figure 2 indicates that the regression coefficients (R^2) are 0.993 and 0.964 for the long-pulse and Q-switched laser configurations, respectively. In both configurations, the regression coefficient is above 0.9 with good linearity. Moreover, it shows better accuracy in the long-pulse laser configuration. The limit of detection can be estimated by the expression $C_L = 3\sigma/k$, where 3σ is the standard deviation of the back-ground with the coefficient 3 and k is the slope of the calibration curve [13]. In long-pulse laser configuration, the standard deviation and the slope are 0.191% and 3.560×10^{-4}, respectively, while they are 0.160% and 2.411×10^{-4} in the Q-switched laser configuration. The limits of detection are 16.096 and 19.909 mg/kg, both below the detection level of natural soil with the long-pulse and Q-switched lasers, respectively, and the limit of detection in the long-pulse laser configuration is 19% less than that in the Q-switched laser configuration.

It can be seen that a better analysis result of the calibration curve for Cr has been obtained with the long-pulse laser. In the long-pulse laser configuration, the power density is 1/800 times and the pulse width is 4000 times of that in the Q-switched laser configuration. Despite the low power density of the laser, the long-pulse laser may be superior in trace element detection by LIBS because of the increase in the plasma lifetime.

Plasma temperature. According to the theory of atomic emission spectroscopy [14], under the assumption of local thermal equilibrium (LTE), the intensity of the spectra can be expressed as

$$I = N_s A g_k e^{-E_k/k_B T}/U_s(T)\,, \qquad (1)$$

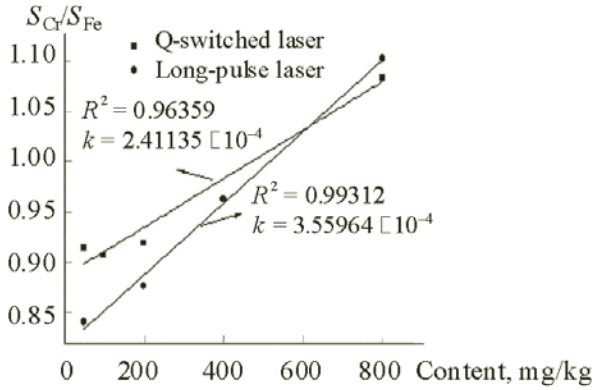

Fig. 2. Signal ratio calibration curves of chromium atomic spectral line at 425.435 nm with the iron reference line at 425.079 nm (S_{Cr}/S_{Fe}) in long-pulse and Q-switched laser configurations.

where I is the intensity of the line, N_s is the emitted particle density, A is the transition probability, g_k is the statistical weight of the upper level, E_k is the energy of the upper lever, k_B is the Boltzmann constant, T is the plasma temperature, and $U_s(T)$ is the partition function. Expression (1) is valid if the self-absorption is negligible. Taking the logarithm of Eq. (1) we obtain the equation

$$\log (I/g_kA) = -E_k/k_BT + \log (FC_s/U_s(T)) , \tag{2}$$

where $\log (FC_s/U_s(T))$ is a constant. After substituting f for A and the value of k_B, we obtain

$$\log (I\lambda^3/gf) = -5040E_k/T + c . \tag{3}$$

In the Boltzmann plot, $\log (I\lambda^3/gf)$ is porportional to E_k (eV) and the slope of the plot ($-5040/T$) is the reciprocal of the plasma temperature. The Boltzmann plot for the five atom lines of Fe (419.910, 425.079, 427.176, 430.790, and 432.576 nm) can be constructed with the long-pulse laser and Q-switched laser configurations. The spectral parameters of Fe I lines can be found on the website of NIST (National Institute of Standards and Technology) [15]. A comparison of the Boltzmann plots calculated in the long-pulse laser and Q-switched laser configuration is shown in Fig. 3. The experiment was reduplicated 10 times in the long-pulse laser and Q-switched laser configurations.

Figure 3 shows that the distribution of data is more concentrated in the long-pulse laser configuration than that in the Q-switched laser configuration. Thus, the spectra induced by the long-pulse laser are more reproducible from shot to shot, and the value of $\log (I\lambda^3/gf)$ in the long-pulse laser configuration is lower compared to that in Q-switched laser configuration, which indicates that the effect of evaporation on the samples is poor and the number of evaporated particles is limited. The slope of the Boltzmann plot yields a plasma temperature of 15795.907 K in the long-pulse laser configuration and 9040.792 K in the Q-switched laser configuration.

Electron density. The line broadening is the result of Doppler broadening, Stark broadening, and broadening of the spectrometer. Self-absorption and Doppler broadening can be neglected in the experiment. The Stark broadening is the mechanism that is taken into account in determining the electron density in plasma, following the equation obtained by H. R. Griem [16]:

$$\Delta\lambda_{1/2} = 2\omega(N_e/10^{16}) + 3.5A(N_e/10^{16})^{1/4}(1 - 1.2N_D^{1/3})\omega(N_e/10^{16}) \text{ (in Å)} . \tag{4}$$

According to Eq. (4), $\Delta\lambda_{1/2}$ is the full width at half maximum of the spectra, $\omega(N_e/10^{16})$ is for electron impact broadening, $3.5A(N_e/10^{16})^{1/4}(1 - 1.2N_D^{1/3})\omega(N_e/10^{16})$ is for ion impact broadening, which can be neglected, ω is electron impact parameter, and A is the ion broadening parameter. Then Eq. (4) can be expressed as

$$\Delta\lambda_{1/2} = 2\omega(N_e/10^{16}) . \tag{5}$$

The atom line of Si at 288.158 nm has been selected for the electron density estimation. The profile of the Stark broadening line is described as the Lorentz function. A comparison of the Stark broadening line at Si I 288.158 nm after Lorentz fitting from soil samples No. 1–5 in the long-pulse laser and Q-switched laser configurations is shown in Fig. 4. It indicates that

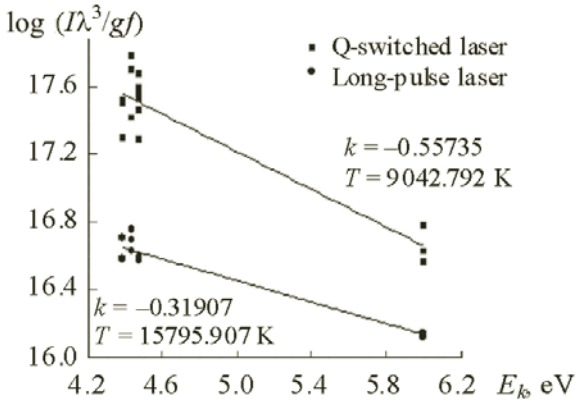

Fig. 3. Comparison of Boltzmann plot calculated for iron lines by long-pulse laser and Q-switched laser.

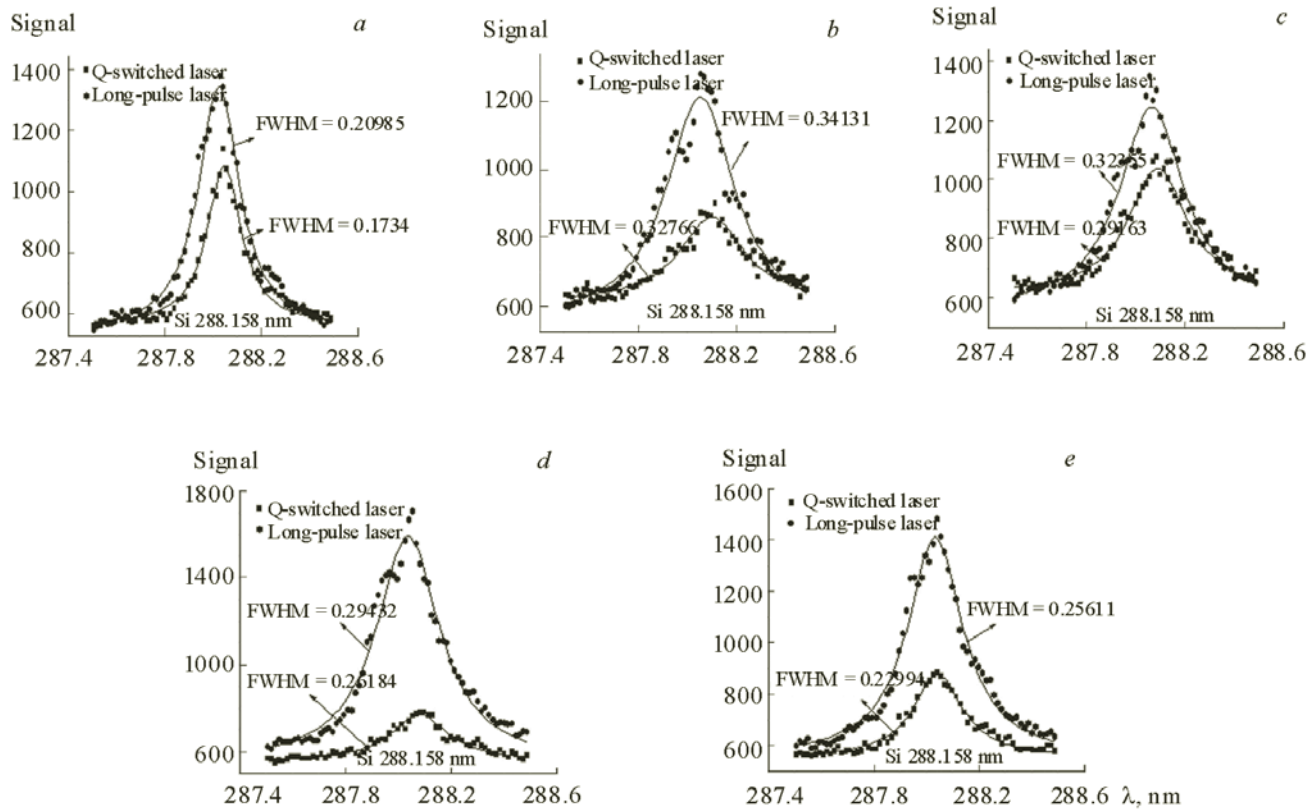

Fig. 4. Comparison of Stark broadening of silicon atomic spectral line at 288.158 nm after Lorentz fitting from soil samples No. 1–5 for the long-pulse laser and Q-switched laser configurations No. 1–5 (a–e).

Stark broadening by a long-pulse laser is greater than by a Q-switched laser. The value of the average value of ω can be obtained from reference data [15]; the average electron density is 2.988×10^{17} and 2.412×10^{17} cm^{-3} for the long-pulse and Q-switched laser configuration.

For analysis of plasma temperature and electron density, the plasma has been assumed to be in LTE. The validity of LTE can be confirmed using Eq. (6) [16]:

$$N_e \geq 1.6 \times 10^{12} \Delta E^3 T^{1/2}, \quad (6)$$

where ΔE is the largest energy transition. In this case, the largest energy transition is 4.3013879 eV at Si I 288.158 nm, and the highest plasma temperature is 15795.907 K. The lowest limit of electron density is 1.6×10^{16} calculated through Eq. (6), which is less than the measured one (2.4×10^{17}) and is consistent with the assumption of LTE in the long-pulse and Q-switched laser induced plasma.

It is found that the intensity of background spectra in the Q-switched laser configuration is stronger than that in the long-pulse laser configuration, but the plasma temperature and electron density in the long-pulse laser configuration is 1.75 and 1.24 times greater than that in the Q-switched laser configuration. It indicates that the evaporation of sample by a long-pulse laser is less than that by a Q-switched laser, while the exciting emission is increased in the long-pulse laser configuration. In conclusion, the plasma temperature and electron density are obviously increased by using the long-pulse laser. The probability of collision of neutral atoms in plasma is increased with increase in laser pulse time. With the enhancement of plasma temperature and electron density, the long-pulse laser has an obvious effect on improving the excitation of plasma and accuracy of analysis of element (Cr).

Conclusions. In the present work, both long-pulse and Q-switched lasers were employed to induce plasmas of Cr-doped reference soil samples. The calibration curve was drawn and plasma parameters (plasma temperature and electron density) were obtained in the long-pulse laser configuration and the Q-switched configuration. The pulse time of the long-pulse laser with a low power density is 4×10^3 times greater than that for the Q-switched laser. Compared to the Q-switched laser configuration, a higher value of R^2 in the calibration curve is obtained, and the limit of detection is decreased 20% in the long-pulse laser configuration, which may have a positive effect of elevating the accuracy of analysis of the element (Cr). Based on the analysis of plasma temperature and electron density, one can conclude that the long pulse time of the laser improves the excitation of the plasma with an increase in the probability of collision and the high kinetic energy of the neutrals in plasma, which improve the analysis by LIBS.

Acknowledgment. This work was supported by the National Natural Science Foundation of China under Grant No. 61378042.

REFERENCES

1. M. A. Gondal, A. Dastageer, M. Maslehuddin, A. J. Alnehmi, and O. S. B. Al-Amoudi, *Opt. Laser. Technol.*, **44**, 566–571 (2012).
2. C. Aragon, J. A. Aguilera, and F. Penalba, *J. Appl. Spectrosc.*, **53**, 1259–1264 (1999).
3. C. Aragon, J. Bengoechea, and J. Aguilera, *Spectrochim. Acta B*, **56**, 619–628 (2001).
4. F. Capitelli, F. Colao, M. R. Provenzano, R. Fantoni, G. Brunetti, and N. Senesi, *Geoderma*, **106**, 45–62 (2002).
5. Z. M. Madhavi, L. Nicole, A. Nicolas, H. Ronny, E. Michael, D. W. Stan, and A. V. Arpad, *Spectrochim. Acta B*, **62**, 1426–1432 (2007).
6. K. Y. Yamamoto, D. A. Cremers, L. E. Foster, M. P. Davies, and P. D. Harris, *Appl. Spectrosc.*, **59**, 1082–1096 (2005).
7. F. C. Alvira, L. Ponce, M. Arronte, and G. M. Bilmes, *J. Phys.*, **247**, 1–6 (2011).
8. L. B. Guo, W. Hu, B. Y. Zhang, X. N. He, C. M. Li, Y. S. Zhou, Z. X. Cai, X. Y. Zeng, and Y. F. Lu, *Opt. Express*, **19**, 14067–14075 (2011).
9. R. Babar, A. Rizwan, A. Raheel, and M. A. Baig, *Phys. Plasmas*, **18**, 1–7 (1994).
10. S. N. Xu, W. Z. Duan, N. R. Bo, Q. Li, A. Zhuo, and R. Jiang, *Spectrosc. Spectral Anal.*, **36**, 1175–1179 (2015).
11. *Environmental Quality Standard For Soil*, GB 15618 (1995).
12. *Plasma Emission Spectrum Analysis*, Beijing, Chemical Industry Press (2005).
13. S. Mohamad and C. Paolo. *Appl. Spectrosc.*, **49**, 499–507 (1995).
14. *Emission Spectral Analysis*, Beijing, Metallurgical Industrial Press (1975).
15. http://www.physics.nist.gov/PhysRefData/ASD/lines_form.html, NIST, National Institute of Standards and Technology for the United States of America.
16. *Plasma Spectroscopy*, McGraw-Hill, New York (1964), pp. 483–521.